

Elastic, electronic, and vibrational properties of RhN compound

E. Deligoz · K. Colakoglu · Y. O. Ciftci

Received: 22 October 2009 / Accepted: 12 March 2010 / Published online: 30 March 2010
© Springer Science+Business Media, LLC 2010

Abstract The structural, electronic, mechanical, and vibrational properties of 4d transition metal mononitride, RhN, are investigated using the norm-conserving pseudo-potentials within the local density approximation (LDA) in the frame of density functional theory. The calculated lattice parameters and the bulk modulus almost agree with the previous theoretical values. The second-order elastic constants have been calculated and the other related quantities such as Young's modulus, shear modulus, anisotropy factor, sound velocities, and Debye temperature also estimated. Charge distributions and density of states are reported to understand the bonding character in the stable phases. We have also obtained the phonon dispersion curves without LO/TO splitting.

Introduction

Transition metal mononitrides are known as refractory compounds, and they have, relatively, high hardness, brittleness, melting point, and superconducting transition temperature, and they also have interesting optical, electronic, catalytic, and magnetic properties [1]. Due to these properties, technological applications are applied widely on them such as diffusion barriers, cutting tools, magnetic storage devices, optical coatings, and hard wear-resistant coatings [2].

E. Deligoz (✉)
Department of Physics, Aksaray University,
68100 Aksaray, Turkey
e-mail: edeligoz@yahoo.com

K. Colakoglu · Y. O. Ciftci
Department of Physics, Gazi University, Teknikokullar,
06500 Ankara, Turkey

Recently, a new material PtN, which is the first binary nitride of the noble metals group, has been synthesized by Gregoryanz et al. [3] using laser-heated diamond anvil-cell techniques at pressures up to 50 GPa and temperatures exceeding 2,000 K. It was found that this compound has a remarkably high bulk modulus of 372 GPa, contrary to the usual behavior of transition metal nitrides. This work shows that the possibility to synthesize other nitrides with notable properties under extreme conditions. After that a large number of works [3–27] have been carried out on their synthesis and on the microscopic understanding of the structural, electronic, elastic, and vibrational properties of them.

RhN, which is a member of the 4d-metal nitrogen compound, has not been synthesized yet. It has been reported only few recent theoretical works on RhN [25–27]. Guillermen et al. [25] studied cohesive properties in the rock-salt structure by using the linear-muffin-tin-orbitals (LMTO) method for this compound. Yu et al. [26] reported that, among the pyrite, rutile, fluorite and marcasite phases, marcasite phase has lower energy for RhN₂. Paiva et al. [27] performed structural, electronic, and magnetic calculations in the zinc-blende structure by using the full potential linearized augmented plane wave method (FP-LAPW) including this compound and reported that, RhN shows a metallic behavior in B3 structure.

To our knowledge, the charge distribution, elastic, and dynamical properties, which are the important bulk properties for solids, have not been considered theoretically for RhN so far. Consequently, the main purpose of this work is to provide some additional information to the existing data on the physical properties of RhN by using the ab initio total energy calculations. Therefore, in this work, we have estimated elastic constants, charge density, Young's modulus, Poisson's ratio, anisotropy factor, sound velocities,

Debye temperature, and phonon frequencies of RhN for the first time. The layout of this article is given as follows: calculations are given in “Method of calculation” section and the results are presented in “Results and discussion” and “Summary and conclusion” sections, respectively.

Method of calculation

The calculations are performed using the density functional formalism and local density approximation (LDA) through the Ceperley and Alder functional [28] as parameterized by Perdew and Zunger [29] for the exchange–correlation energy in the SIESTA code [30, 31]. This code calculates the total energies and atomic forces using a linear combination of atomic orbitals as the basis set. The basis set is based on the finite range pseudoatomic orbitals (PAOs) of the Sankey_Niklewsky type [32], generalized to include multiple-zeta decays.

The interactions between electrons and core ions are simulated with separable Troullier–Martins [33] norm-conserving pseudopotentials. We have generated atomic pseudopotentials separately for atoms, Rh and N by using the $5s^14d^8$, and $2s^22p^3$ atomic configurations, respectively. The cut-off radii are taken as 2.18 au for s, p, d, and f channels for Rh and 1.24 au for s, p, d, and f channels au for N. Relativistic effects are taken into account for Rh due to its heavy mass in the pseudopotential calculations.

Siesta calculates the self-consistent potential on a grid in real space. The fineness of this grid is determined in terms of an energy cut-off E_c in analogy to the energy cut-off when the basis set involves plane waves. Here, by using a double-zeta plus polarization orbitals (DZP) basis and the cut-off energies between 100 and 350 Ry with various basis sets, we found its optimal value around of 300 Ry. Atoms were allowed to relax until atomic forces were less than 0.04 eV \AA^{-1} . For final convergence, 256 k -points in B1 and B3 structures, 405 k -points in B2 structure, and 160 k -points in B4 structure were enough to obtain the converged total energies ΔE to about 1 meV/atom for present compound.

Results and discussion

Structural properties

For RhN, four structures, which are rock-salt (B1), cesium chloride (B2), zinc-blende (B3), and wurtzite (B4), are considered. The bulk moduli and its pressure derivative have been computed minimizing the crystal total energy for different values of the lattice constant by means of Muraghan’s equation of state (eos) [34] as in Fig. 1. The order

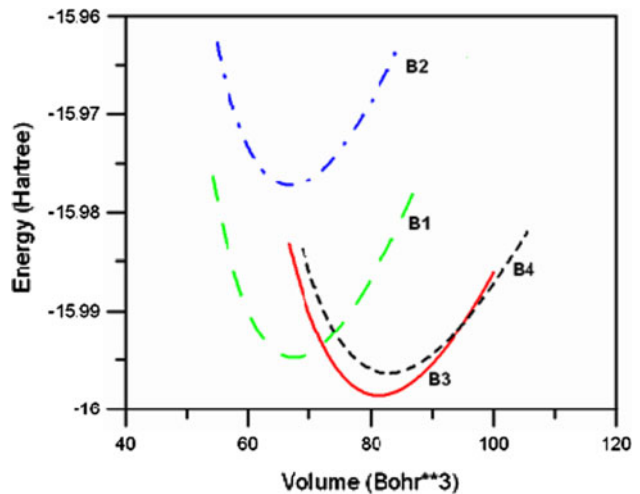


Fig. 1 (Color online) Energy versus volume curves of RhN (per atom)

of energetic stability of phase structures of RhN from high to low is: B3 < B4 < B1 < B2. These inequalities show that the B3 phase has the lowest energy among them. Since the total energy difference between B4 and B3 phases is 0.00446 Hartree (per atom), B3 phase can easily transform to B4 structure for RhN.

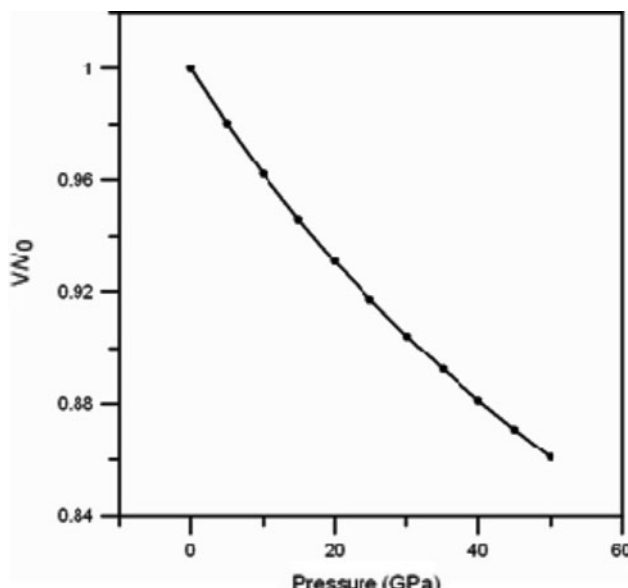
Table 1 shows the calculated lattice constants, internal parameter, bulk modulus, and first pressure derivative of bulk modulus for each phase of RhN together with the other theoretical values [25, 27]. The lattice parameters (a) are found to be 4.58, 4.31, 2.71, and 3.27 Å for B3, B1, B2, and B4 structures, respectively. The calculated lattice constants are higher (1 and 5% for B3 and B1 structure, respectively) than other theoretical findings in Refs. [25, 27]. These small deviations may be explained by using different approximations in the density functional methods.

The B3 structure has the largest lattice constant (4.58 Å) and B2 structure has the smallest (2.71 Å) one for this compound. The lattice constant for the B1 structure is slightly smaller than that for B3 structure. Because, in B3 structure the N atoms are located at the tetrahedral site of the face-centered-cubic structure of the Rh atoms, and this site is rather closer to neighboring transition metal atoms as compared to the octahedral site of the N atoms in the B1 structure [27]. In all calculations we have used the computed lattice parameters.

In the present case, the calculated bulk moduli are 240.78, 273.89, 269.84, and 215.86 GPa for B3, B1, B2, and B4 structures, respectively. Therefore, the order of compressibility from high to low is: B4 > B3 > B2 > B1. For these configurations, the largest value of bulk modulus (273.89 GPa) is obtained for B1 structure, and this is slightly higher than that for B2 structure (269.84 GPa). The values of the bulk moduli indicate that RhN is the least

Table 1 The calculated equilibrium lattice constant (a_0), bulk modulus (B), the pressure derivative of bulk modulus (B'), internal parameter (u), and cohesive energy (E_{coh}) together with the theoretical values for RhN

	Zinc-blende	Rock-salt	Cesium chloride	Wurtzite
RhN				
a (Å)	4.58 (4.51 ^a)	4.31 (4.08 ^b)	2.71	0.27
c (Å)	—	—	—	5.26
u	—	—	—	0.374
c/a	—	—	—	1.607
B (GPa)	240.78 (267.85 ^a)	273.89	269.84	215.86
B'	4.15	4.30	4.45	4.91
E_{coh} (eV/atom)	−13.03	−11.94	−11.80	−12.04

^a FP-LAPW within LSDA (Ref. 27)^b LMTO within LSD (Ref. 25)**Fig. 2** The ratio V/V_0 versus pressure curves in ZB structure

compressible material in the B1 structure. The bulk modulus for B3 structure is lower (about 10%) than the other theoretical result given in Ref. [27].

The ratio V/V_0 , as a function of the applied pressure, is given in Fig. 2 for B3 structure. It is seen that, when the pressure increases from 0 to 50 GPa, the ratio of V/V_0 decreases. The reason of this changing can be attributed to the atoms becoming closer in the interlayer and having stronger interactions.

The cohesive energy is known as a measure of the strength of the forces which bind atoms together in the solid state. In this connection, the cohesive energy of RhN is calculated. The cohesive energy (E_{coh}) of a given phase is defined as the difference in the total energy of the constituent atoms at infinite separation and the total energy of that particular phase:

$$E_{coh} = E_{\text{RhN}} - E_{\text{Rh}} - E_{\text{N}_2}/2 \quad (1)$$

The energy calculations for both pure constituent atoms and compound have to be performed at the same level of accuracy so as to obtain a precise value for the cohesive energy [35]. Energy of an isolated atom is calculated by considering a supercell containing an isolated atom. This is achieved by using the spin dependent form of functional, with atoms in the ground-state spin configuration. The computed cohesive energies (E_{coh}) are found to be −13.03, −11.94, −11.80, and −12.04 eV/atom for B3, B1, B2, and B4 structure, respectively, and they are also listed in Table 1.

Elastic properties

The elastic constants of solids provide a link between the mechanical and dynamical behavior of crystals, and give important information concerning the nature of the forces operating in solids. In particular, they provide information on the stability and stiffness of materials, and their ab initio calculation requires precise methods. Since the forces and the elastic constants are functions of the first-order and second-order derivatives of the potentials, their calculation will provide a further check on the accuracy of the calculation of forces in solids. They also provide valuable data for developing inter atomic potentials.

Here, to compute the elastic constants (C_{ij}), we have used the “volume-conserving” technique [36], as in our recent works [24, 37], and the findings are shown in Table 2. Unfortunately, there are no theoretical results for

Table 2 Elastic constants (in GPa) for RhN

Structure	C_{11}	C_{12}	C_{44}
B3	293.27	258.30	19.26

comparing with the present work. Then, our results can serve as a prediction for future investigations.

For a stable cubic structure, the three independent elastic constants C_{ij} (C_{11} , C_{12} , and C_{44}) should satisfy the well known Born–Huang criteria for stability

$$(C_{11} - C_{12}) > 0, \quad C_{11} > 0, \quad C_{44} > 0, \\ (C_{11} + 2C_{12}) > 0.$$

The present elastic constants in Table 2 obey these stability conditions for B3 structure.

The Zener anisotropy factor (A), which is an indicator of the degree of anisotropy in the solid structure. For a completely isotropic material, the A factor takes the value of 1, when the value of A smaller or greater than unity it is a measure of the degree of elastic anisotropy. Poisson's ratio (v), shear modulus (G), and Young's modulus (E), which are the most interesting elastic properties for applications, are often measured for polycrystalline materials when investigating their hardness. These quantities are calculated in terms of the computed data using the following relations [38]:

$$A = \frac{2C_{44}}{C_{11} - C_{12}}, \quad (2)$$

$$v = \frac{1}{2} \left[\frac{(B - \frac{2}{3}G)}{(B + \frac{1}{3}G)} \right], \quad (3)$$

and

$$E = \frac{9GB}{G + 3B} \quad (4)$$

where $G = (G_V + G_R)/2$ is the isotropic shear modulus, G_V is Voigt's shear modulus corresponding to the upper bound of G values and G_R is Reuss's shear modulus corresponding to the lower bound of G values; they can be written as

$$G_V = \frac{(C_{11} - C_{12} + 3C_{44})}{5} \quad (5)$$

$$5/G_R = 4/(C_{11} - C_{12}) + 3/C_{44} \quad (6)$$

for the cubic system.

Another important parameter is the Kleinman parameter (ζ) which describes the relative positions of the cation and anion sublattices under volume conserving strain distortions for which positions are not fixed by symmetry. We use the following relation [39] for this purpose:

$$\zeta = \frac{C_{11} + 8C_{12}}{7C_{11} + 2C_{12}} \quad (7)$$

The calculated Zener anisotropy factor, Poisson's ratio, Kleinman parameter, Young's modulus, and isotropic shear modulus for B3 structure are shown in Table 3. The calculated Zener anisotropy factor is close to the value of 1.

Table 3 The calculated Zener anisotropy factor (A), Poisson's ratio (v), Kleinman parameter (ζ), Young's modulus (E), and isotropic shear modulus (G) for RhN

Structure	A	v	ζ	E (GPa)	G (GPa)
B3	1.11	0.46	0.91	54.19	18.52

This shows that the RhN is an elastically isotropic compound. Fu et al. [40] and Yoo [41] are reported that the large values of Zener anisotropy factor can give rise to the driving force (tangential force) acting on screw dislocations to promote the cross-slip pinning process. The $v = 0.25$ and 0.5 are the lower limit and upper limit for central force solids, respectively [40]. Our v values are close to the value of 0.4 indicating the interatomic forces are predominantly central forces in the RhN.

Young's modulus is defined as the ratio of stress and strain, and used to provide a measure of the stiffness of the solid. The material is stiffer if the value of Young's modulus is high. Since the present value of Young's modulus (54.2 GPa) for RhN is low, this material will not be stiffer.

It is known that isotropic shear modulus and bulk modulus are a measure of the hardness of a solid. The bulk modulus is a measure of resistance to volume change by applied pressure, whereas the shear modulus is a measure of resistance to reversible deformations upon shear stress [42]. Therefore, isotropic shear modulus is better predictor of hardness than the bulk modulus. The calculated isotropic shear modulus is 18.52 GPa for B3 structure. We conclude that RhN is a sort of highly compressible compound. According to the criterion [42, 43], a material is brittle (ductility) if the B/G ratio is less (high) than 1.75. The value of the B/G is high 1.75 for RhN in B3 structure. Hence, this material behaves in a ductility manner.

The Debye temperature is known as an important fundamental parameter closely related to many physical properties such as specific heat and melting temperature. At low temperatures the vibrational excitations arise solely from acoustic vibrations. Hence, at low temperatures the Debye temperature calculated from elastic constants is the same as that determined from specific heat measurements. We have calculated the Debye temperature, θ_D , from the elastic constants data using the average sound velocity, v_m , by the following common relation given in Ref. [44]

$$\theta_D = \frac{\hbar}{k} \left[\frac{3n}{4\pi} \left(\frac{N_A \rho}{M} \right) \right]^{1/3} v_m, \quad (8)$$

where \hbar is Planck's constant, k is Boltzmann's constant, N_A is Avogadro's number, n is the number of atoms per formula unit, M is the molecular mass per formula unit, $\rho = M/V$ is the density, and v_m is given [45] as

Table 4 The longitudinal, transverse, and average elastic wave velocities, together with the Debye temperature, for RhN

Structure	Reference	v_l (m/s)	v_t (m/s)	v_m (m/s)	θ_D (K)
B3	Present	5730.1	1513.2	1727.2	224.63
	Theory ^a (RS structure)				392

^a Ref. [25]

$$v_m = \left[\frac{1}{3} \left(\frac{2}{v_t^3} + \frac{1}{v_l^3} \right) \right]^{-1/3}, \quad (9)$$

where v_l and v_t , are the longitudinal and transverse elastic wave velocity, respectively, which are obtained from Navier's equation [46]:

$$v_l = \sqrt{\frac{3B+4G}{3\rho}}, \quad (10)$$

and

$$v_t = \sqrt{\frac{G}{\rho}}. \quad (11)$$

The calculated values of the longitudinal, transverse, and average sound velocities in the present formalism are shown in Table 4 along with the Debye temperature. The calculated Debye temperature in B3 phase is lower than that for in B1 phase given by Ref. [23].

Electronic properties

We have also, predicted the band structure for RhN in the zinc-blende structure along the high-symmetry directions in the first Brillouin zone from the calculated equilibrium lattice constant. It can be seen from the Fig. 3 that there are

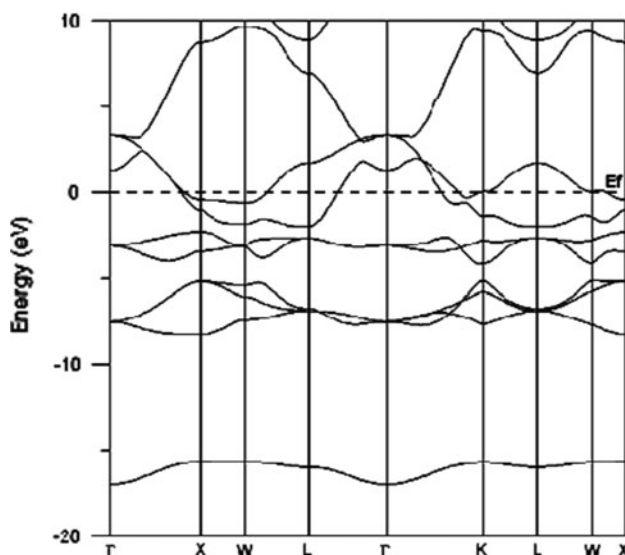


Fig. 3 The calculated band structures of RhN for ZB structure. The position of the Fermi level is at 0 eV

three bands crossing at the Fermi level, and this band structures exhibit a metallic character (no band gap). The present band profiles agree well with the earlier work [25].

The total and partial density of states (DOS and PDOS) corresponding to the band structures shown in Fig. 3 are, also, indicated in Fig. 4 along with the Fermi energy level. The position of the Fermi level is at 0 eV. In this figure, the lowest valence bands occur between about -17 and -15 eV and are essentially dominated by N-2s states. The other valence bands are essentially dominated by Rh-4d states. The 2p and 2s states of N atoms are also contributing to the valence bands, but the values of densities of these states are quite small compared to Rh-4d. The energy region just above Fermi energy level are dominated by unoccupied Rh-4d states. These results indicate that there is a strong hybridization between the N states and Rh states.

To visualize the nature of the bonding character, charge-density distributions in (100) plane for zinc-blende structure is shown in Fig. 5. It can be seen that there is an increase of the electron density around the N atoms, and a decrease in the interstitial region between Rh atoms where the metal–metal bonding have formed. We note that the difference of the electro negativity between Rh and N appears in the difference of the charge transfer. These imply that beside the strong covalent interaction, an ionic contribution to the bonding mechanism exists in the Rh–N system. Therefore, the bonds are an unusual mixture of metallic, covalent, and ionic bondings.

Phonon dispersion curves

Energy dispersion of phonons provides important information about the dynamical properties [47] of materials. In particular, it is an essential in calculation of specific heat, sound velocity, thermal expansion, heat conduction, vibrational entropy, free energy via quasiharmonic approximation, infrared and Raman absorption, electron–phonon interaction, etc. In addition, low frequency modes can be associated with phase transformations, while imaginary frequencies show that the calculated structure is not the most stable [48].

The present ab initio code, SIESTA, and its VIBRA package by Ordejon calculate the phonon frequencies without LO/TO splitting by using the Hellmann–Feynman forces on atoms in supercell. At the minimized state all

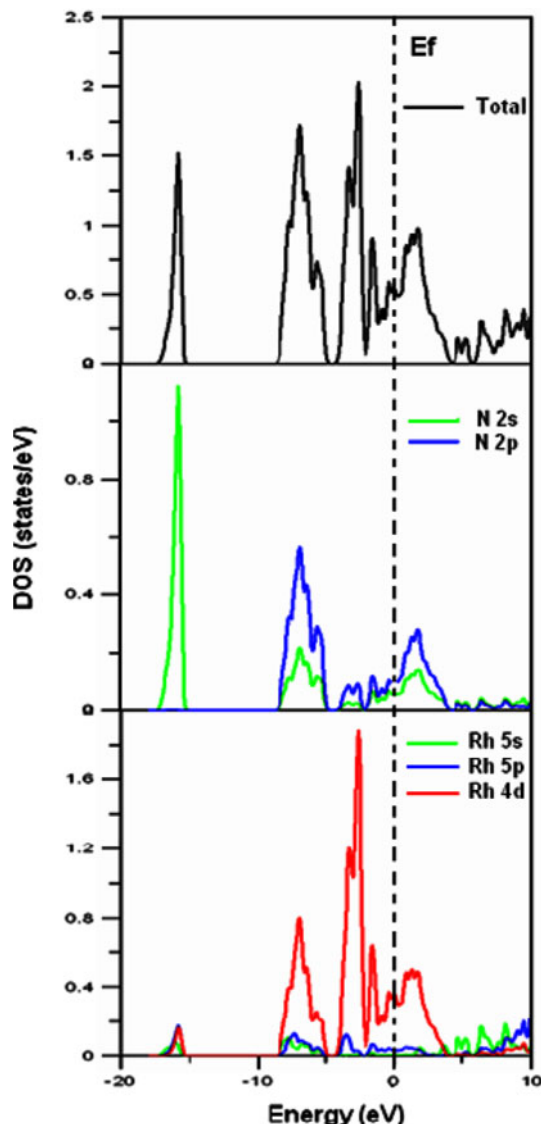


Fig. 4 (Color online) The calculated total DOS and atomic projected DOS of RhN for ZB structure. The position of the Fermi level is at 0 eV

Hellmann–Feynman forces are desired to be vanished. Within the same programs the Hellmann–Feynman forces are calculated for the related configuration with single atom displaced from equilibrium position, and in terms of the force constants and dynamical matrix the required phonon frequencies are evaluated in usual manner. Specifically, we have calculated the phonon dispersion curves in high-symmetry directions for $1 \times 1 \times 1$ cubic supercell with 54 atoms. The displacement amplitudes are taken as 0.04 Bohr.

The present phonon dispersion curves for RhN along the high-symmetry directions are illustrated in Fig. 6. As expected, the large gaps occur between the optic and acoustic modes due to the big mass ratio ($m_{\text{Rh}}/m_{\text{N}} = 7.35$) of constituent atoms (cation and anion). The value of this

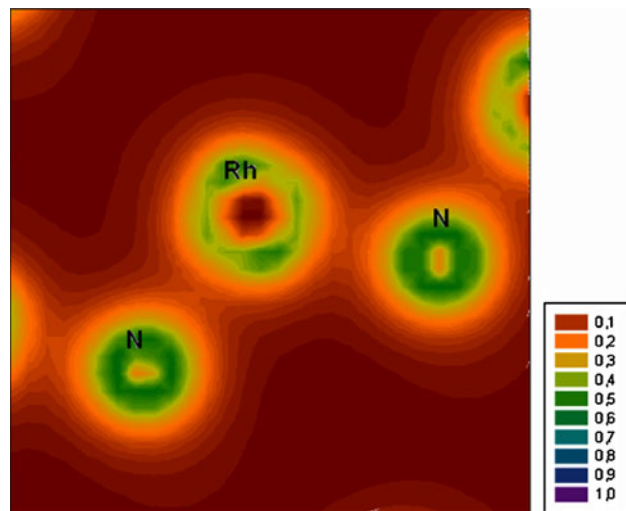


Fig. 5 (Color online) Charge-density distributions in (100) plane for ZB structure

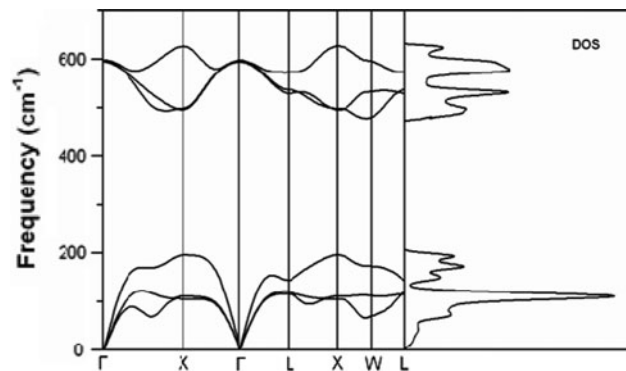


Fig. 6 The phonon dispersion curves and density of state of RhN in ZB structure

gap is about 138.33 cm^{-1} at X point. The absence of imaginary frequencies (soft modes) in the phonon dispersion curves strongly supports the dynamically stable character of B3 phase. Also, as is expected, RhN is metallic character in B3 structure, longitudinal optical and transverse optical phonon modes are triple degenerate at the zone center.

The corresponding one-phonon density of state (DOS) is also depicted for RhN at the right-hand-side of the same Fig. 6. A sharp peak near 100 cm^{-1} is characterized by acoustic region due to transverse acoustic (TA) branches crossing along the [100] and [111] symmetry directions.

Summary and conclusion

In this work, we have performed ab initio total energy calculations on RhN in the rock-salt, cesium chloride, zinc-blende and wurtzite structures. We have revealed that the

zinc-blende phase is in the ground-state configuration and the band structures of this phase are metallic in nature. Beside the other contributions, the original aspects of the present calculations concern the charge density, phonon dispersion curves, elastic and thermodynamical findings, which have not been considered so far. Our results for elastic constants satisfy the traditional mechanical stability conditions for B3 phases. Since there are no experimental data available for this hypothetical compound, we think that the ab initio theoretical estimation is the only reasonable tool for obtaining such important information.

Acknowledgements This work is supported by Gazi University Research-Project Unit under Project No: 05/2009-55. Finally, we kindly acknowledge Dr. Savas Berber for helping on the charge-density calculations.

References

1. Gubanov VA, Ianovsky AL, Zhukov VP (1994) Electronic structure of refractory carbides and nitrides. Cambridge University Press, Cambridge
2. Toth LE (1974) Transition metal carbides and nitrides. Academic Press, New York
3. Gregoryanz E, Sanloup C, Somayazulu M, Badro J, Fiquet G, Mao H-K, Hemley RJ (2004) Nat Mater 3:294
4. Young FA, Montoya AJ, Sanloup C, Lazzari M, Gregoryanz E, Scandolo S (2006) Phys Rev B 73:153102
5. Yu R, Zhang XF (2005) Appl Phys Lett 86:121913
6. Sahu BR, Kleinman L (2005) Phys Rev B 71:041101R
7. Uddin J, Scuseria GE (2005) Phys Rev B 72:035101
8. Yu R, Zhang XF (2005) Phys Rev B 72:054103
9. Fan CZ, Sun L, Zhang J, Jia Y, Wei Z, Liu R, Zeng S, Wang W (2005) Chin Sci Bull 50:1079
10. Kanoun MB, Goumri-Said S (2005) Phys Rev B 72:113103
11. Kanoun MB, Goumri-Said S, Jaouen M (2007) Phys Rev B 76:134109
12. Kutolin SA, Belova LF, Samoilova RN, Kotenko OM (1976) Izv Akad Nauk SSSR Neorg Mater 12:1585
13. Peng F, Fu H, Yang X (2008) Physica B 403:2851
14. Patil SKR, Khare SV, Tuttle BR, Bording JK, Kodambaka S (2006) Phys Rev B 73:104118
15. Kim O, Achenbach JD, Mirkarimi PB, Shinn M, Barnett SA (1992) J Appl Phys 72:1805
16. Yang Q, Lengauer W, Koch T, Scheerer M, Smid I (2000) J Alloys Compd 309:L5
17. Lu X, Selleby M, Sundman B (2007) Acta Mater 55:1215
18. Ojha P, Aynya M, Sanyal SP (2007) J Phys Chem Solids 68:148
19. Amrani B, El Haj Hassan F (2007) Comput Mater Sci 39:563
20. Isaev EI, Simak SI, Abrikosov IA, Ahuja R, Vekilov YKh, Katsnelson MI, Lichtenstein AI, Johansson B (2007) J Appl Phys 101:123519
21. Chen XJ, Struzhkin VV, Wu Z, Somayazulu M, Qian J, Kung S, Christens AN, Zhao Y, Cohen RE, Mao H-K, Hemley RJ (2005) Proc Natl Acad Sci USA 102:3198
22. Cheng D, Wang S, Ye H (2004) J Alloys Compd 377:221
23. Kanoun MB, Goumri-Said S (2007) Phys Lett A 362:73
24. Deligöz E, Çolakoğlu K, Çiftçi YO (2008) Chin Phys Lett 25:2154
25. Guillermet AF, Haglund J, Grimvall G (1992) Phys Rev B 45:11557
26. Yu R, Zhan Q, De Jonghe LC (2007) J Solid State Chem 45:1136
27. de Paiva R, Nogueira RA (2007) Phys Rev B 75:085105
28. Ceperley DM, Alder MJ (1980) Phys Rev Lett 45:566
29. Perdew P, Zunger A (1981) Phys Rev B 23:5048
30. Ordejón P, Artacho E, Soler JM (1996) Phys Rev B (Rapid Commun) 53:R10441
31. Soler JM, Artacho E, Gale JD, García A, Junquera J, Ordejón P, Sánchez-Portal D (2002) J Phys Condens Matt 14:2745
32. Sankey OF, Niklewski DJ (1989) Phys Rev B 40:3979
33. Troullier N, Martins JL (1991) Phys Rev B 43:1993
34. Murnaghan FD (1944) Proc Natl Acad Sci USA 30:5390
35. Ahmed R, Hashemifar SJ, Akbarzadeh H, Ahmed M, Alem F (2007) Comput Mater Sci 39:580
36. Wang SQ, Ye HQ (2003) J Phys Condens Matter 15:5307
37. Deligöz E, Çolakoğlu K, Çiftçi YÖ, Özışık H (2007) J Phys Condens Matter 19:436204
38. Mayer B, Anton H, Bott E, Methfessel M, Sticht J, Schmidt PC (2003) Intermetallics 11:23
39. Harrison WA (1989) Electronic structure and properties of solids. Dover, New York
40. Fu H, Li D, Peng F, Gao T, Cheng X (2008) Comput Mater Sci 44:774
41. Yoo MH (1986) Scr Metall 20:915
42. Shein IR, Ivanovskii AL (2008) J Phys Condens Matter 20:415218
43. Pugh SF (1954) Philos Mag 45:833
44. Johnston I, Keeler G, Rollins R, Spicklemire S (1996) Solid state physics simulations, the consortium for upper-level physics software. Wiley, New York
45. Anderson OL (1963) J Phys Chem Solids 24:909
46. Schreiber E, Anderson OL, Soga N (1973) Elastic constants and their measurements. McGraw-Hill, New York
47. Bruesch P (1982) Phonons: theory and experiment. Springer, New York
48. Ackland GJ, Warren MC, Clark GJ (1997) J Phys Condens Matter 9:7861